

On the Origin of Shrimpluminescence

Tyler C. Sterling*

(Dated: January 5, 2022)

[illegible]

I. INTRODUCTION

Snapping shrimp, like our cute friend in Fig. 1 (left), have long been known to produce cavitating bubbles by *snapping* their claws [1; 2; 3]. They have a strong appendage (the *dactyl*) in thier claw [Fig. 1 (center)] that is used to create a very high-velocity jet of water. The low pressure region in the jet’s wake forms a bubble [Fig. 1 (t=0 ms)] that, among other things, produces an exceptionally loud noise when it collapses. The sound (i.e. the pressure wave) produced by even a *single* shrimp’s snap is detectable over a mile away [4]. The noise produced by groups of shrimp is so intense that the U.S. Navy used them as “sonar-camouflage” in the Pacific ocean during World War II [1].

The shrimp were not patriots helping the war-effort, however; they snapped for food. The shock-wave produced by the cavitating bubble is used to stun and even kill prey [1]. If the shrimp’s prey had very sensitive eyes (and also were not dead) they might notice a flash of light is also produced through an effect referred to as “shrimpoluminescence” in the case of the pistol shrimp [2], but more generally known as *sonoluminescence*.

Sonoluminescence (SL) is more precisely defined as the process by which a “driven gas bubble collapses so strongly that the energy focusing at collapse leads to light emission” [5]. Sonoluminescence comes in two forms: (i) single-bubble sonoluminescence and (ii) multi-bubble sonoluminescence. The distinction is self-explanatory: multi-bubble sonoluminescence (MBSL) consists of “the simultaneous creation and destruction of many separate, individual cavitation bubbles” [5; 6], whereas in single-bubble sonoluminescence (SBSL), rather obviously, only a single bubble is present [7]. The discovery of MBSL predates SBSL by ~ 60 years but due to the more-or-less random and fleeting nature

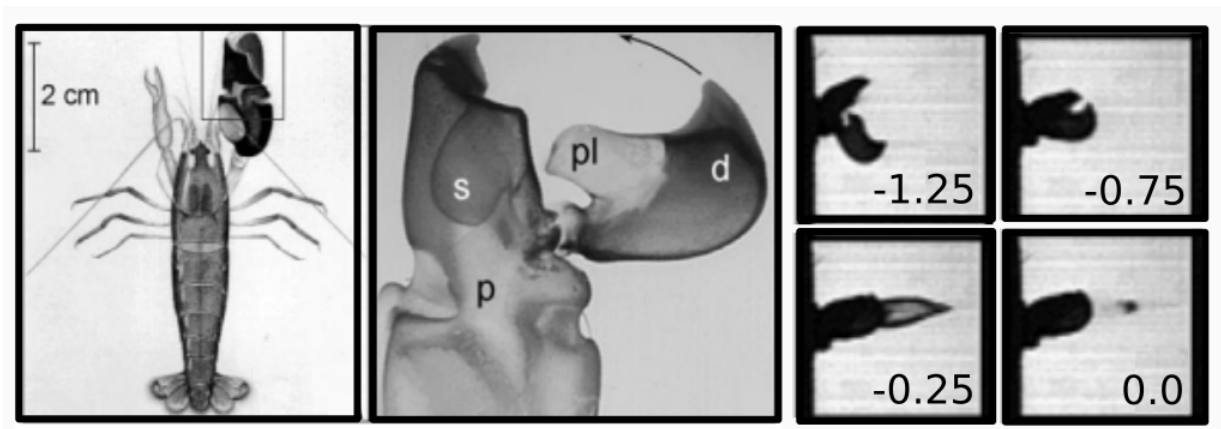


FIG. 1 (left) Snapping shrimp (*Alpheus heterochaelis*). (center) Blown-up view of the shrimp's claw. The *plunger* (pl) on the *dactyl* (d) rapidly enters the *socket* (s), ejecting a high-velocity jet of water. The water ejection and subsequent bubble formation and, finally, bubble collapse (at $t=0$) are shown on the right. The time-offset are shown in the panels in ms. Adapted from ref. [1]

* ty.sterling@colorado.edu

of the bubbles, SL in general wasn't well studied until the early 1990's when it was discovered that single bubbles could be created and periodically driven to produce light with very high precision [5; 6; 7; 8]. We will discuss MBSL briefly throughout this paper, but for now it suffices to say that nearly all theoretical and experimental progress to explain sonoluminescence has been made using SBSL, with some authors even calling it "the hydrogen atom of sonoluminescence" [6; 9].

In SBSL, emission from a single bubble is not complicated from multiple scattering (off other bubbles), volumetric-light emission from the bubble cloud, etc. Similarly, the bubble is not perturbed by interaction with other bubbles and, due to its tiny size, by interaction with the container walls and the theory is greatly simplified compared to MBSL. SBSL, while offering advantages, also comes with complications. Due to the tiny volume of the bubble, directly measuring the temperature or pressure *inside* the bubble is practically impossible [10]. Still, the discovery of SBSL created a rush of effort to explain the phenomena with arguments ranging from the simplest models ¹ to more exotic explanations based of quantum field theory [11; 12; 13].

But besides the obvious case of shrimpluminescence, why is SL interesting? Well, at a glance, it is not obvious why SL occurs. The acoustic wave in the liquid displaces molecules on the order of nanometers, costing an elastic energy of $\sim 1 \times 10^{-12}$ eV/molecule while emitting visible light (through e.g. electronic transitions) costs an energy ~ 1 eV/molecule [6; 9]... there is a 12-orders-of-magnitude concentration of energy. That is huge! Estimates of the temperature at the center bubble are ...

After 3 decades of studying SBSL, the physical mechanism of light production in SL is still not understood. This can be seen by glancing at the literature and noticing that there are many recent papers with different arguments for *where* ² the light comes from [14; 15; 16; 17]. Numerous aspects of the process are conveniently accessible to the experimentalist, while at the same time the theory of the bubble's interior is quite mature. Many theories require experimental inputs as parameters, while in other cases experimental results are indirectly *inferred* by fitting to a theory. Put simply, the history of studying SBSL is a rather beautiful example of the scientific process of explaining nature. According to Brenner "SBSL has become a rather sophisticated testing ground for the ability of mathematical models and numerical simulations to explain detailed experimental data from a complicated physical process" [5].

The goal of this paper is to catch the reader up on recent efforts to explain SBSL. While the author of this paper is particularly excited about shrimpluminescence, it is important to stress that this work will focus on SBSL in general. It is apparently simpler to create and characterize SBSL in the laboratory without involving shrimp (for example, convincing the shrimp to snap requires tickling them [1; 2; 9]), so practically all work to study SL has not involved shrimp ³. Also notably absent will be any detailed discussion of MBSL since this will take us too far afield. Instead, we will summarize the history of SBSL research up to now starting at the discovery of MBSL leading to the subsequent discovery of SBSL and a rush of effort to explain it. We will explore both the experimental and theoretical discoveries along the way. Finally, we will review the current state of agreement between what is known experimentally and theoretically about SBSL.

II. HISTORICAL OVERVIEW

SL was discovered by accident in 1933 (in the form of MBSL) by Marínescu and Trillat [18] and was subsequently characterized by Frenzel and Schultes [19] ⁴ Marínescu et al. were trying to accelerate photo development by *insonating* developing fluid. They discovered that a photosensitive plate immersed in the insonated fluid became "foggy" which they attributed to exposure to light. Shortly after, Frenzel et al. repeated the experiment and confirmed that the insonated fluid emits light in the form of a faintly glowing cloud of bubbles.

This result was not particularly surprising to the community since it had been known for a while that cavitating bubbles could do tremendous damage to e.g. ship's propellers ⁵. The discovery's impact is concisely summarized by Brenner: "if the cloud [of cavitating bubbles] collapses violently enough to break molecular bonds in a solid, why should it *not* emit photons" [5]. In fact, cavitating bubbles had been of interest to engineers working on fluid mechanics for a while. The discovery of cavitation is credited to Euler (as early as 1754) who hypothesized that if the velocity in a fluid was large enough, negative pressures could become so large as to "break the fluid" [7; 20]. Cavitation was confirmed to exist (and named "cavitation") in 1895 by engineers studying the failure of a British

¹ There are far too many to try list here and we will not be interested in the vast majority of early models which are now irrelevant. References to these can be found in Gaitan [8] and Brenner et al. [5].

² We emphasize "where" since it's not even certain if the light is *surface* or *volumetric* emission, i.e. it is literally not known *where* the light comes from [].

³ With notable exceptions [3]

⁴ Neither the paper due to Marínescu et al. nor the one due to Frenzel et al. can be found by the author; in any case he can't read French or German so having the papers wouldn't be much use. As such, the story of how the effect was discovered is taken from more recent sources whose authors hopefully could read French and German [5; 6; 8]

⁵ A more modern example could be my van's oil pump, which is in need of replacing.

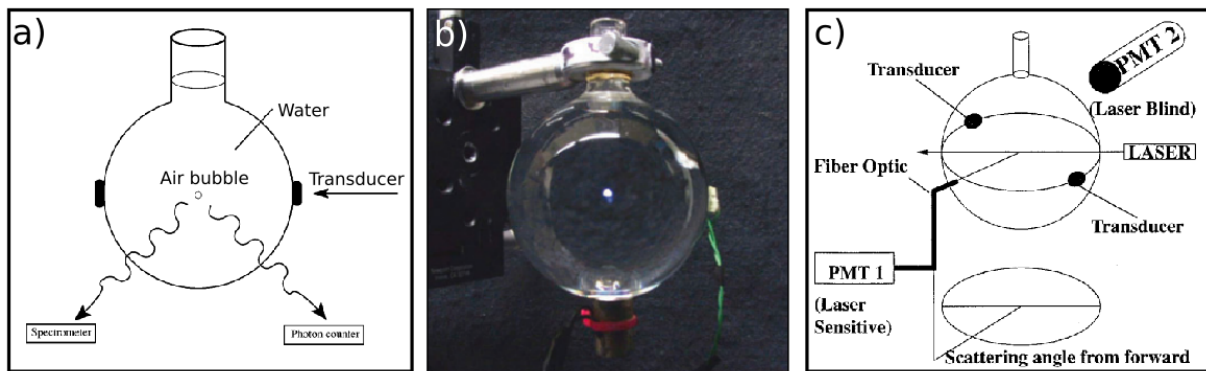


FIG. 2 (a) Schematic of a spherical acoustic levitation cell. The piezoelectric transducers that drive the bubble trapped in the flask are labeled in the diagram. (b) Photograph of the same. Here, the fluid is aqueous H_2SO_4 instead of water. A sonoluminescing bubble is clearly visible in the center of the flask. The photo was taken in a fully lit room with exposure time 2 s. (c) Schematic of a Mie scattering experimental setup. A similar acoustic levitation cell as (a) is shown with an added laser source and photomultiplier tubes (PMT) to analyze the scattered and emitted light. (a), (b), and (c) are from refs. [5], [10], and [28] respectively.

Navy ship's propeller [20]. Shortly after, Lord Rayleigh wrote down and solved the differential equation for a vapor filled cavity collapsing in water (the so-called Rayleigh equation), giving the first rigorous theoretical treatment of cavitation [21; 22]. Rayleigh found that, for a bubble at a lower pressure than the surrounding fluid (and both pressures held constant), the bubble wall diverges during collapse. Still, very little information was accessible about the light emission until the 1990's when stable⁶, single bubbles could be created and driven to emit light [6; 7; 8]. With this discovery, serious interest took root.

Details of a typical SBSL experiment will be given later, but for now it suffices to note that SBSL, unlike previous studies on MBSL, allowed very precise control and measurement of the SL process. With unprecedented experimental control, many discrepancies in previous assumptions about SL were discovered. Experimental Results measuring the duration of the light pulse found that it was orders of magnitude smaller than the time in which the bubble was compressed to its smallest radius [23; 24]. This discovery implied that SL was nearly decoupled from the bubble's dynamics, contradicting models based on Rayleigh's equation. New models were proposed based on *converging shock waves* at the bubble's center with estimates of the temperature at the center of bubbles $\sim 10^8$ K [25; 26]. At the same time, experimentalists fit the bubble's light emission spectra as a *black body emitter* and concluded that the temperature in the bubble was at least 25,000 K [27].

These very high estimates for the temperature in the bubbles lead to a spark of interest more broadly: if the temperature in the bubble were really that large, then it should be possible for nuclear *fusion* to occur [7]. An action movie featuring Keanu Reeves was even made with this at the center of the plot⁷. In the early 2000's, several papers were even published claiming that stable nuclear fusion was possible in the lab using a method based on SBSL [7]. Unfortunately these results turned out to be fraudulent [7]. Shortly after this fiasco, evidence emerged that there are shape instabilities in the bubbles dynamics indicating that the converging shock-wave hypothesis is probably not right. This severely reduced the estimates for the temperature to below 10,000 K, ruling out the possibility of fusion occurring at all [7]. Moreover, it was shown that the light is most likely emitted from the *bulk* of the bubble as opposed to its surface, making fits to a black body spectrum (i.e. surface emission) incorrect [7]. Current estimates for the temperature at the center of a sonoluminescing bubble are ... [7]

Still, the very high pressures and temperatures in the bubble during sonoluminescence see technological applications in chemistry and biosciences. ...

History has shown that the most important part of understanding SBSL is understanding the dynamics of a single acoustically driven bubble. We will see that the dynamics of the gas *inside* the bubble is nearly decoupled from the dynamics of the *fluid* containing the bubble so that we may look at these two problems separately. Firstly, we look at the problem of the fluid containing the bubble; we will derive the equations of motion for the bubble's wall. Next, we will use our results for the bubble's wall to understand the dynamics of the gas trapped in the bubble. After that,

⁶ *Stable* is compared with *transient* when discussing cavitation. A stable bubble persists through multiple cycles of cavitation, oscillating nonlinearly around an equilibrium size. Transient bubbles appear and then collapse to disappear

⁷ It is called *Chain Reaction* and I am unwilling to watch it.

we will combine these two and discuss solutions of the full problem. The ultimate result of this will turn out to be an estimate of the *temperature* in the bubble. We will then look at theories presenting the origin of light from the very hot contents of the bubble. Finally, we will wrap this whole thing up with a summary of unsolved problems and an outlook to the future.

III. BUBBLE DYNAMICS

The conditions in the bubble’s *interior* are still not entirely understood and will be the subject of an entire subsection of this paper. Before we get to this, we will at an older problem: the dynamics of a periodically driven bubble in a liquid. An important aspect of the bubble’s dynamics is that they are experimentally accessible. Moreover, as we shall see, a (relatively) simple theory describes the dynamics of the bubble quite well. On the other hand, measuring what is going on in the bubble’s interior is not at all simple though much progress has been made theoretically.

A. The Bubble Wall

As it turns out, the dynamics of the bubble in SBSL (regardless of the light emission) are quite well described both qualitatively and *quantitatively* by the classical theory of bubble dynamics [5; 10; 22; 29; 30; 31; 32]. This isn’t particularly surprising since the light emission and bubble collapse occur at different timescales (the duration of maximum compressions is $\sim 0.003\%$ of the bubble’s period) [5; 10; 22; 29; 30]. The starting point for any theory of the bubble dynamics is Rayleigh’s original work [21], now expounded upon by many others. The most widely known modern work is that of Plesset [22; 30; 33], resulting in the so called “the Rayleigh-Plesset” (RP) equation. The derivation assumes the host liquid is incompressible, ultimately resulting in us neglecting the effects of sound radiated by the bubble. Corrections exist that improve upon the RP equation in various ways and we will discuss these below []. However, for brevity’s sake, we will only derive the RP equation here and merely quote the others as they are very similar in form to the RP equation. The field of *bubble dynamics* is quite mature and attempting to review it here would be out of scope of this paper; instead, the reader is referred to numerous books and reviews [].

The RP equation can be deduced from the *Navier-Stokes* (NS) equations ⁸ [5; 10; 22; 29; 30; 31]. The NS equations for a compressible fluid are

$$\begin{aligned} \rho \frac{d\mathbf{u}}{dt} &= \rho [\partial_t \mathbf{u} + (\mathbf{u} \cdot \nabla) \mathbf{u}] = -\nabla p + \eta \nabla (\nabla \cdot \mathbf{u}) + \mu \nabla^2 \mathbf{u} + \mathbf{f}_B \\ \partial_t \rho + \nabla \cdot (\rho \mathbf{u}) &= 0. \end{aligned} \tag{1}$$

Here, $\mathbf{u}(\mathbf{x}, t)$ is the velocity of a fluid parcel at position \mathbf{x} at time t , $\rho(\mathbf{x}, t)$ is the fluid’s density, p is the pressure, $\eta \equiv (\xi + \frac{2}{3}\mu)$ is the *bulk* viscosity with μ the *shear* viscosity, and \mathbf{f}_B are *body* forces (e.g. gravity, electrostatic forces) which are usually from external sources and will be assumed negligible from here on. The subscripts on ∂ denote what derivative is being taken and ∇ and ∇^2 have their usual meanings. The first equation is *conservation of momentum* for the fluid, i.e. Newton’s 2nd law; the second equation is *mass conservation*. The total-derivative of a moving fluid $\frac{d}{dt} \equiv D_t$ is sometimes called the *material derivative*. In the case of velocity $D_t \mathbf{u}$ is the *acceleration* of the fluid. It records not only explicit time dependence of the fluid’s velocity $\partial_t \mathbf{u}$ but also how the fluid’s velocity varies *in space* as it moves past us: $(\mathbf{u} \cdot \nabla) \mathbf{u}$. The pressure term on the right hand side is to be understood as forces from the *elastic* energy. On the other hand, the terms $\sim \mathbf{u}$ are viscous (damping) terms that tend to make the velocity field spatially uniform: they vanish when the (spatial) derivatives of the velocity vanish. The bulk-viscosity term $\sim \eta$ damps radial changes in the fluids velocity (e.g. dilation/contraction) while the shear-viscosity term $\sim \mu$ resists shearing.

Solving eqs. 1 is an intractable problem. To make progress, we will make some drastic approximations that are more-or-less valid for our problem. Firstly, we will assume irrotational flow (i.e. $\nabla \times \mathbf{u} \equiv 0$) so that there is only radial motion in the liquid (i.e. $\mathbf{u} = u\mathbf{r}$). Note that, since the flow is assumed irrotational, we can represent the velocity as the gradient of a scalar function: $u\mathbf{r} = \partial_r \phi \mathbf{r}$ [34]. This amounts to assuming that the bubble is always spherical which seems like a rather drastic approximation but has been validated experimentally in many cases []. The fact that the bubble tends to remain spherical can be understood by accounting for surface-tension at the liquid-bubble interface [29].

⁸ The NS equations are derived in the appendix

Nextly, we assume that the viscous terms are negligible in the bulk dynamics of the liquid. For (relatively) low viscosity fluids such as water which is also nearly incompressible, this is an accurate approximation and is widely used [5; 22; 29; 30]. We will account, to some extent, for viscosity later when looking at the bubble-liquid interface. Moreover, we are assuming that the flow is *isentropic*, i.e. that it is reversible (no damping) and that no heat is exchanged between fluid parcels. We will further assume that the liquid is isothermal, i.e. its temperature is constant (in space). Then pressure p is determined from an instantaneous equation-of-state $p = p(\rho, T)$. In the case of SBSL, this is valid since the bubble makes up a *tiny* fraction of the total volume and, as we will later see, heat-transport across the liquid-bubble interfacing is usually neglected anyway (i.e. the bubble is compressed adiabatically in the thermodynamic sense ⁹).

Lastly, related to the fact that the bubble is tiny, we assume that the extent of the liquid is so large compared to the bubble that we may consider the dynamics of the liquid as if there were no bubble present; similarly, we consider the dynamics of a bubble in an infinite, isotropic medium. Of course the bubble-liquid interface enters both systems as a boundary condition [30].

With these simplifying assumptions (and a vector identity ¹⁰) we rewrite eqs. 1 as a system of 1 + 1 dimensional partial differential equations:

$$\begin{aligned} \partial_r \left[\partial_t \phi + \frac{1}{2} (\partial_r \phi)^2 \right] &= -\frac{1}{\rho} \partial_r p \\ \partial_t \rho + \partial_r \phi \partial_r \rho + \rho \partial_r^2 \phi &= 0. \end{aligned} \quad (2)$$

We can integrate the first equation above using the fact that the compressibility is negligible to move the density through the integration [35]

$$\int_{r_\infty}^r \frac{\partial}{\partial r'} \left[\partial_t \phi + \frac{1}{2} \left(\frac{\partial \phi}{\partial r'} \right)^2 \right] dr' = -\frac{1}{\rho} \int_{r_\infty}^r \frac{\partial p}{\partial r'} dr'. \quad (3)$$

On the left side, we take the velocity to vanish at infinity. On the right side, we assume that only the static and unperturbed pressures, p_∞ and $P(t)$ respectively, are relevant so that [29; 30; 35]

$$\partial_t \phi + \frac{1}{2} (\partial_r \phi)^2 = \frac{(p_\infty + P(t)) - p(t, r)}{\rho}. \quad (4)$$

Eq. 4 gives the pressure at coordinate (r, t) in terms of the velocity of the fluid, the density, and the applied pressure.

Now, let us assume that the velocity potential satisfies a wave equation $\nabla^2 \phi - \frac{1}{c^2} \partial_t^2 \phi = 0$ ¹¹ with c the speed of sound in the fluid. Again, we use incompressibility by recalling that for an incompressible fluid $c \rightarrow \infty$ which implies $\nabla^2 \phi = 0$ ¹². In this case, we can ignore retardation effects and, remembering that we have spherical symmetry, write the solution of $\nabla^2 \phi$ as

$$\phi = \frac{\psi(t)}{r} \quad (5)$$

with ψ the time-dependent coefficient. We now use the boundary condition for the velocity at the bubble wall, $u(R) \equiv \dot{R}$ with R the bubble radius, to determine ψ :

$$\dot{R} = -\frac{\psi}{R^2} \Rightarrow \psi = -R^2 \dot{R}. \quad (6)$$

Thus, we find $\phi(r, t) = -\frac{R^2 \dot{R}}{r}$. Plugging this into the left hand side of eq. 4 and evaluating at the bubble wall, $r \equiv R$

$$\begin{aligned} \partial_t \phi|_{r=R} &= -2\dot{R}^2 - R\ddot{R} \\ \partial_r \phi|_{r=R} &= \dot{R} \equiv u(R) \end{aligned} \quad (7)$$

⁹ According to Wikipedia, *adiabatic* means *fast* in thermodynamics lingo. This is relevant to us since we are claiming the bubble wall moves so quickly that it is compressed to its maximum pressure before any heat can flow out. On the otherhand, the mechanics lingo implies *adiabatic* to mean *slow*. This is, e.g. the adiabatic theorem in quantum mechanics: a perturbation acts so slowly that the system is in its groundstate at all times.

¹⁰ $(\nabla \cdot \mathbf{u}) \mathbf{u} = \frac{1}{2} \nabla(u^2) - \mathbf{u} \times (\nabla \times \mathbf{u})$

¹¹ This doesn't come from thin air. We could write the r.h.s. of eq. 4 as the enthalpy, $h \equiv \int \frac{dp}{\rho}$, and similarly introduce $dh = \frac{dp}{\rho}$ in the first line of eq. 2. Eliminating h between the two and dropping small terms $\sim \frac{u}{c}$, we arrive at the homogeneous wave equation [5; 29; 35].

¹² For our problem, it is true that $(\frac{1}{c^2} \partial_t^2 \phi) / \nabla^2 \phi \sim \left(\frac{R}{\lambda} \right)^2 \ll 1$, i.e. the long wave-length approximation is accurate [29; 30; 35].

Finally, sticking all this together, we arrive at the Rayleigh-Plesset equation [22; 29; 30; 33; 35]

$$R\ddot{R} + \frac{3}{2}\dot{R}^2 = \frac{p_B(t) - (p_\infty + P(t))}{\rho} \quad (8)$$

with $p_B \equiv p(r = R, t)$ the pressure in the fluid at the bubble wall. Evaluated beyond the bubble wall, $r > R$, eq. 8 gives the pressure radiated by the fluctuating bubble. Some comments are in order. The combination $p_\infty + P(t)$ is the *ambient* pressure [29; 30] which gives the pressure in the fluid in the absence of the bubble. The left hand side of eq. 8 may be regarded as the kinetic energy (density). The right hand side is the change in enthalpy (density) due to the fluctuating bubble, i.e. the dynamics of the bubble given on the left hand side are determined by the enthalpy in the fluid due to the bubble's motion. In deriving this equation, we have assumed that the speed of propagation in the fluid is infinite. In reality, this is not true but this approximation will be very good close to the bubble (in the *near-field*) where retardation effects are negligible anyway. In a similar way, we have assumed that the energy in the fluid due to distorting its volume is negligible. This approximation will be accurate near the bubble as well since the kinetic energy in this region will dominate [29].

We can refine eq. 8 a little further. Since the motion in the fluid is purely radial, we expect the only relevant stresses to be normal to the bubble wall. Let's denote the radial stress in the liquid at some point r by $s_r(r) = -p(r, t) + 2\mu\partial_r u$. Recall, μ is the fluid viscosity from earlier. Using conservation of mass and momentum, and our expression above for the velocity, we can equate the normal stresses in the fluid to those in the bubble:

$$s_r(R) = -p_B - 4\frac{\mu\dot{R}}{R} = -p_g + 2\frac{\sigma}{R} \quad (9)$$

where p_g is the pressure in the gas and σ is the surface tension. Solving for $p_B(t)$, we have the relation [5; 29; 30]

$$p_B(t) = p_g(t) - \frac{1}{R} (2\sigma + 4\mu\dot{R}). \quad (10)$$

Note that in deriving the equations 2 we neglected the viscosity terms. This was valid since only combinations of viscosity and compressibility $\nabla \cdot \mathbf{u}$ appeared, both of which are assumed small. Here, however, we opt to keep the viscosity terms coupling the bubble wall to the fluid. With this, we can rewrite the RP equation as

$$R\ddot{R} + \frac{3}{2}\dot{R}^2 = \frac{1}{\rho} \left[\Delta p(t) - \frac{1}{R} (2\sigma + 4\mu\dot{R}) - P(t) \right] \quad (11)$$

with $\Delta p = p_g(t) - p_\infty$ the deviation of the pressure inside the bubble from the static pressure. With the above assumption that the compression is adiabatic, the conditions inside the bubble are decoupled from the liquid (besides the coupling through the RP equation) and we may regard $p_g(t)$ in the bubble as a given quantity to be determined from an equation of state. Recall $P(t)$ is the time-dependent part of the pressure in the absence of the bubble: we may regard this as an external pressure from e.g. a driving stress. This will be from the transducers driving the acoustic levitation cell.

Eq. 11 is the equation of motion for a driven spherical bubble in an infinite, incompressible fluid. It is worth briefly summarizing this all again. On the left hand side, R is the radius of the bubble, \dot{R} is the velocity of the bubble's radius i.e. the velocity of the *bubble wall*, and \ddot{R} is the bubble wall's acceleration. On the right hand side, ρ is the (constant) density of the fluid. $\Delta p(t) = p_g(t) - p_\infty$ is the deviation of the gas pressure in the bubble, $p_g(t)$, from the static fluid pressure at infinite distance, p_∞ . $p_g(t)$ is evaluated at the bubble wall. In the second term, the $\sim \sigma$ part gives the restoring force from surface tension stresses while the $\sim \mu$ term is due to the fluid viscos stresses: σ and μ are the surface tension and viscosity coefficients respectively. The last term on the right, $P(t)$, is the *external pressure*. For problems relevant to SBSL, the driving pressure, $P(t)$ in the RP equations, is an acoustic plane wave. Keller and coworkers showed that the modification required to the RP equations result in the replacement $P(t) \rightarrow P_0 \sin(\omega t)$ [36]. If we linearize in the bubble's radius $R(t) \approx R_0 (1 + x(t))$ with $x(t) \ll 1$, we can derive a forced harmonic oscillator equation for $x(t)$ [31; 32]. However, the low driving amplitude regime where this method is valid is irrelevant to SBSL so we won't pursue it here.

Let us briefly digress to discuss retardation effects. If we had not assumed incompressibility, our solution would include a term arising from the sound radiation from the bubble itself. There are practical issues with this solution however; it is *third* order in time and has unphysical, exponentially diverging solutions [5; 29; 30; 37]. Both issues are solved by imposing boundary conditions on the \ddot{R} term. The method for doing so is also challenging and apparently no unique way to do it exists [30; 38; 39]. Instead, there is a whole family of solutions that can be derived; different

variations of the improved RP equation, which are collectively referred to as “Rayleigh-Plesset equations” are derived by neglecting different terms in the full compressible solution. We will discuss this again below.

The RP equation (eq. 11) is pretty but its analytical solution intractable. Direct solutions of the RP equation or its variants are done numerically using e.g. the Euler method [31; 40]. It is no great challenge computationally. For now, let’s see what we else we can understand from this analytically by making some more approximations. If we take $p_B - (p_\infty + P) \equiv p_0$ with p_0 constant, we recover Rayleigh’s equation discussed above [5; 21; 29; 33]. This is valid during the part of the bubble’s cycle called *The Rayleigh collapse*: when the bubble’s wall is very fast, the \dot{R}^2 term will be much larger than the right hand side of eq. 11 and we may neglect it. Rayleigh looked at the same problem, i.e. a cavitating *void* in water, by replacing $p_0 \rightarrow 0$ [5; 21]:

$$R\ddot{R} + \frac{3}{2}\dot{R}^2 = 0 \quad (12)$$

which has a solution that diverges as $R(t) \sim [(t_* - t)/t_*]^{2/5}$ [5]. This observation is what lead to Rayleigh’s argument for the origin of cavitation damage to ship’s propellers. Yasui gave a rather elegant heuristic explanation for the origin of *cavitation* in a fluid that is worth stating here [31]. Consider the mass flowing through concentric shells around a bubble, $4\pi R_i^2 v_i \rho$. For a source free field, we require that neighboring shells satisfy conservation of mass: $4\pi R_1^2 v_1 = 4\pi R_2^2 v_2$. For $R_2 > R_1$, we see that $v_1/v_2 = (R_2/R_1)^2$. The velocity for a smaller radius is always larger, diverging towards the origin.

In reality, the bubble’s velocity does not become infinite and, in the case of *stable* SBSL, the radius remains finite at all times. In the full RP equation (eq. 8) the only term capable of compensating the bubble wall’s motion is the diverging pressure inside the bubble itself [5]. Applying the same analysis to the family of solutions derived when including the bubble’s sound radiation, it turns out that the most important term for slowing the bubble wall’s diverging velocity is $\propto \dot{p}_g$. Keeping only this term, we arrive at the most popular variant of the RP equation [41; 42]:

$$R\ddot{R} + \frac{3}{2}\dot{R}^2 = \frac{1}{\rho} \left[\Delta p(t) - \frac{1}{R} (2\sigma + 4\mu\dot{R}) - P(t) + \frac{R}{c} \dot{p}_g \right]. \quad (13)$$

This equation is only slightly more complicated than the RP equation (eq. 11), the only change being the added term $\propto \dot{p}_g$ which is determined from solving the decoupled problem of the gas inside the bubble. Eq. 13 is usually solved numerically; we will look at results of numerical solutions later when talking about experiments. For now, we note that the observed error between this equation and experiment is only significant in the interval during bubble collapse and even still, results of solving this equation are quantitatively in good agreement with measurements of the bubble’s radius [5].

B. The Bubble’s Interior

The theoretical progress on the bubble’s interior since the discovery of SBSL in the late 1990’s [7] follows two paths [5; 10; 31]: (i) model calculations based on the RP equations and an equation of state for the pressure (i.e. the temperature) are used to try to reproduce the easily measurable dynamics of the bubble. (ii) We can model the light emission itself and compare our calculation to spectroscopic measurements of SBSL []. Obviously these are related topics, but the distinction in the context of SBSL is important as we will now see.

Most early progress on the bubble’s interior depended on the former method: if we predict the right dynamics, then we might know the correct pressure and temperature in the bubble. These data are then used to try to describe the light emission []. This was preferred to studying the emitted spectra directly as careful measurements resulted in an almost featureless spectrum that could not be explained []. Calculating the dynamics of the bubble’s wall from the RP equations (eq. 11 or eq. 13) requires the pressure inside the bubble as input. We would like to find a suitable form for $\Delta p(t) \sim p_g(t)$ in the RP equations that reproduces the measured radius-time curve $R(t)$ for a stable cavitating bubble. It turns out that this is a very hard problem for a number of reasons: the conditions inside the bubble depend on gas diffusion and rectification (one-directional diffusion) between the liquid and the bubble, water-vapor condensation and evaporation inside the bubble, and chemical reactions between species in the bubble [5]. Brenner et. al elegantly summarized the impact of the problem [5]: “one of the exciting features of modern research on SBSL is that it is a testing ground for how well mathematical models can deal with such a complicated situation”

Now let us briefly discuss the bubble’s light spectrum. For the first decade or so, SBSL experiments were done using partially degassed water as the liquid medium [5; 7; 10]. Careful measurements of the emission from SBSL in water resulted in an almost featureless spectrum []. Early attempts were made to fit this as black-body radiation resulting

in *huge* temperature estimates, e.g. 10^8 K []. It was later discovered that SBSL is volume emission, indicating that black-body radiation is not valid []. Little progress was made on this front for quite some time [5]. The utility of analyzing the light spectrum of SBSL in water is succinctly described by Suslick [10]: “because of the inherent ambiguity associated with the analysis of featureless spectra of unknown origin, a more rigorous explanation is unlikely to be generated”.

SBSL was first measured in partially degassed water [5; 7; 8]¹³ Early attempts to understand the physics required exploring the phase-space over which SBSL occurs. Some attempts were made using non-aqueous host liquids e.g. alcohols, silicone oils [42; 43], but experiments with air bubbles were not very successful [42]. Instead, different gases were tried in water. Recall, air is $\sim 80\%$ N_2 , $\sim 20\%$ O_2 , and $\sim 1\%$ Ar. Considering the relatively large content of O_2 and N_2 , degassed water *regassed* with N_2 or O_2 or a mixture were checked first and found not to produce SBSL [44]. What was discovered was that a small amount of *noble gas* was required for SBSL to occur [5; 42; 44]. A result of this work was the *argon rectification hypothesis* [5; 10; 31; 45]. The hypothesis claims that all species (in air) in the bubble besides argon are gradually ejected from bubble’s interior until all that remains is pure argon. The theory is based on the fact that, at the elevated temperatures and pressures inside the bubble, dissociation of O_2 and N_2 into radicals is possible. These species then react with the water vapor radicals to form species that are soluble in the host fluid. As the pressure becomes very large during the compression stage of SBSL, the soluble materials leave the bubble and do not re-enter since their solubility in water is enormous compared to the Ar content of the bubble [45]. Over many cycles, the contents of the bubble become nearly pure argon. Moreover, it was realized that the SBSL was much more intense when the contents of the bubble are a pure inert gas: if the contents were e.g. molecules, bond breaking/formation would alter the pressure of the gas, ultimately reducing the temperature and reducing the light production [5; 9; 10; 31]. This mechanism has been used to explain the relatively weak light, i.e. the low temperature, in MBSL: the bubbles are transient and cannot remove a significant amount of O_2 or N_2 over a single cycle. The current belief is that the contents of a bubble in SBSL are pure argon after $\sim 10^3$ cycles [5; 31].

Most studies continued to use water as the host liquid until it was realized that SBSL in aqueous H_2SO_4 produces light 10^3 times brighter than in water, allowing more precise measurements of the light spectrum []. More importantly, new measurements revealed the phase space of SBSL in aqueous H_2SO_4 included a much larger range of pressures than water. Careful experiments revealed that the spectrum depended critically on the noble gas content and driving pressure. Suslick et. al measured the different emission spectra from Ar, Xe, and Kr bubbles in aqueous H_2SO_4 [10; 46; 47]. Importantly, they were able to identify spectral lines from Ar^+ , Xe^+ , and Kr^+ excited state transitions, proving that the core of the bubble is plasma. Perhaps equally as crucially, they found the *absence* of emission lines from components of aqueous H_2SO_4 vapor [10; 47; 47]: the plasma contained only the noble gas, experimentally confirming the argon rectification hypothesis. Moreover, the spectra at different pressures were in very good agreement with detailed calculations of emission from noble gas plasmas [48; 49]. Increased pressure results in increased collision rate between particles, broadening the excited state transition spectral lines [10; 46; 47; 49]. Further calculations showed that the greatly increased viscosity and density of aqueous H_2SO_4 , $\sim 10\times$ and $\sim 1.3\times$ larger than that of water, lead to reduced (by orders of magnitude) pressure in the bubble at the same driving pressures [48]. The larger pressure in the bubbles in water was found to be consistent with the featureless emission spectrum [10; 31].

This argon rectification hypothesis greatly helped to refine models for the gas dynamics in the bubble and clarified several unexplained experimental observations [5; 10]. With this in mind, we choose only to focus on results known to be relevant to the dynamics of a bubble undergoing SBSL. Excellent books and modern reviews on modelling the gas dynamics exist elsewhere [5; 31; 32]. We will hold off on discussing the dynamics in the plasma until a later section.

C. Gas Dynamics

The most straightforward way to model the gas dynamics in the bubble is through direct solution of the Navier-Stokes equations for the gas [5]. In fact, serious quantitative predictions of the conditions of the bubble’s interior take this path [46; 47; 48; 49; 50]. With simplifying assumptions, equations of motion with varying degrees of sophistication can be derived for the gas and the system of gas dynamical equations and the RP equations are solved numerically. The discussion proceeds in much the same way as deriving the RP equations above but is considerably more complicated [5; 31], so we will omit it here. An important aspect of these studies is the understanding of why relatively simple models work quite well. We will highlight the salient features before introducing a simple model for the gas that will enable us to gain some physical understanding analytically. An especially important result of

¹³ Degassing lowers the ambient pressure, making it easier for bubbles to form.

direct numerical solution of the gas dynamics was (theoretical) confirmation of the argon rectification hypothesis [], reducing the possible gas dynamical models to those applicable to a monatomic gas. Various other models fully including dissipation and heat transport into/out of the bubble showed that the bubble's compression is, to a good approximation, adiabatic and quasistatic []. Before we turn to discuss a model for the gas dynamics, let us pause to mention that another theoretically appealing method for modelling the gas dynamics is *molecular dynamics* []. While this method is attractive for a number of reasons, practical calculations containing realistic numbers of particles aren't possible, limiting the applicability [5].

A simple but reasonable model for the gas dynamics in the bubble is that of an adiabatically, quasistatically compressed ideal gas [5]¹⁴. Let us remind ourselves what the pressure is in this case. Suppose that we have a volume, V , of an ideal gas containing N particles at a temperature T . The ideal gas law tells us the equation of state is $PV = Nk_B T$ with k_B Boltzmann's constant. Since we are assuming adiabatic compression, the second law of thermodynamics tells us that $dU = -PdV$ with U the internal energy in the gas. Moreover, we may use the equipartition theorem to write $dU = Nfk_B dT/2$ with f the number of *degrees of freedom* per particle []. Recall that for an ideal gas []:

$$\begin{aligned} C_V &= \frac{Nfk_B}{2} \\ C_P &= C_V + Nk_B \\ \frac{C_P}{C_V} &= 1 + \frac{f}{2} \equiv \Gamma \end{aligned} \tag{14}$$

with C_V and C_P the heat capacities at constant volume and pressure respectively. For a monatomic ideal gas, $f = 3$ and $\Gamma = 5/2$. Now we can use the second law of thermodynamics to write $C_V dT = -PdV$. From the equation of state, we have

$$dT = \frac{PdV + VdP}{Nk_B} = \frac{PdV + VdP}{C_P - C_V}. \tag{15}$$

Eliminating dT and simplifying,

$$\frac{dP}{P} = -\left(\frac{C_P}{C_V}\right) \frac{dV}{V} = -\Gamma \frac{dV}{V}. \tag{16}$$

Integrating eq. 16, we find

$$P_2 = P_1 \left(\frac{V_1}{V_2}\right)^\Gamma \tag{17}$$

where P_2 is the pressure in a gas at volume V_2 that was initially contained in a volume V_1 at pressure P_1 . Importantly we have not made any assumptions about the shape of the container.

Let us now connect this to the problem of SBSL. In our case, we assume that our bubble has an *ambient* radius R_0 , leading to volume $V_0 = 4/3\pi R_0^3$. Similarly, we will assume the pressure in the bubble at ambient radius R_0 is known and we will call it p_0 . What we want to calculate is the pressure in the gas as a function of the bubble's radius $R(t)$ determined from the RP equations (eq. 11 or eq. 13). Earlier we called the pressure in the gas $p_g(t)$ and we will stick with this here. Plugging these into eq. 17, (and sneaking in a modification) we arrive at a very commonly used equation in the context of SBSL [5; 41; 42; 52]:

$$p_g(t) = p_0 \left(\frac{R_0^3 - h^3}{R^3(t) - h^3}\right)^\Gamma \tag{18}$$

The new variable h that was added willy-nilly is called the *Van der Walls hard-core radius* and its purpose is to make sure that, if the bubble collapses so strongly that its contents become incompressible (i.e. $R(t) \rightarrow h$), the pressure diverges [5; 52]. Eq. 18 can be inserted into an RP equation which can then be integrated numerically to determine the bubble's dynamics. Now recall that one of main goals of modelling the bubble dynamics in SBSL was to calculate

¹⁴ Actually we want to study a *Van der Walls* gas, but we will sneak this aspect in later. The modifications to the result for an ideal gas are simple [51].

the temperature inside the bubble in order to model the light emission. Following similar steps to deriving $p_g(t)$, we can write down an equation for the temperature T [5; 42]:

$$T(t) = T_0 \left(\frac{R_0^3 - h^3}{R^3(t) - h^3} \right)^{\Gamma-1}. \quad (19)$$

Of course we still have to assign a reasonable guess to T_0 , the temperature in the bubble at ambient radius R_0 .

Our physical intuition tells us why eq. 18 is sensible during the bubble's collapse: the bubble wall's velocity is fast and very little heat can flow out during compression. Detailed calculations starting from the full NS equations further tell us that the gas dynamics in the bubble can be regarded as *quasistatic* []. During the expansion and afterbounce stages of the bubbles cycle, which comprise its majority, the gas dynamics should instead be regarded as *isothermal*. This is true because, when the bubble's velocity is on the order of the *heat diffusion* timescale, the temperature throughout the bubble is nearly equal to that in the liquid [5; 29; 31]. The relevant modifications to eq. 18 turns out to be replacing $\Gamma \rightarrow 1$. A neat way of including both isothermal and adiabatic gas dynamics is continuously varying the exponent, Γ in eq. 18, between its adiabatic and isothermal values, C_P/C_V and 1, respectively. A summary of this work is given in refs. [5] and [29]. It turns out that this process doesn't result in better quantitative predictions since, during the assumed isothermal part of the process, dissipation becomes important [5]. It is also possible to include heat and mass diffusion in simple model forms and these do give slightly improved quantitative agreement with experiment; however we choose to discuss solutions of the RP equations using the simpler form given in eq. 18 as this will enable to understand the important features of the bubble's cycle. More advanced solutions using the full gas dynamical equations are qualitatively similar [5; 31].

D. Experimental Results

Creating stable, single bubbles in a laboratory experiment is not particularly challenging and can be done with standard and low-cost materials ¹⁵. A typical experimental setup is shown in Fig. 2. Since we are mainly concerned with the light emission process itself, we will only sketch the experimental setup; it can be summarized as follows [5; 7; 8; 10; 28; 31; 32; 53]. A sample of degassed liquid is placed into a flask ¹⁶. Coupled to the outside of the flask are piezoelectric transducers of some sort. The piezos are driven by a sinusoidal function generator to excite an acoustic resonance of the flask: a typical flask is a few cm across with a resonance at ≈ 20 kHz [5]. The frequency is chosen to form a pressure *antinode* at the center of the flask.

Let us take a brief aside: in deriving the RP equations, we assumed the center of the bubble was stationary. Actually, this is what we want in an SBSL experiment and it is worth discussing under what conditions this is true. In an ideal, incompressible fluid the net force acting on a bubble may be written as

$$\mathbf{f} = - \int_{\partial\Omega} p \mathbf{n} dA = - \int_{\Omega} \nabla p dV \quad (20)$$

Here, \mathbf{f} is the net force, p is the pressure at the bubble's surface, \mathbf{n} is the unit normal vector point out of the bubbles surface, and $\partial\Omega$ is the bubble's boundary with Ω the bubble's domain. The last term is due to an application of Gauss's theorem. Bjerknes [54] took $\nabla p \equiv \nabla p(r=0, t)$ to be constant and averaged over one period of oscillation to find

$$\mathbf{f} = -\frac{4}{3}\pi \langle R^3 \nabla p \rangle. \quad (21)$$

This is the so called *Bjerknes force*. The point is that if the bubble is located at a pressure extrema, e.g. the center of the flask, then this force should vanish and the bubble will remain stationary, an essential result for SBSL experiments.

Some authors have looked at corrections to the bubble's dynamics in the presence of bouyancy, which causes a net translation other than the Bjerknes force. The result is the bubble oscillates around an equilibrium position near but away from the center of the flask [55; 56; 57]. The translational motion of the bubble leads to shape distortion which is beleived to suppress SL; this is confirmed by SBSL experiments in microgravity resulting in larger intensity light production [55].

¹⁵ Actually, the phase-space for SBSL is "small". The coordinates being driving amplitude, driving frequency, fluid composition, temperature, ambient pressure, gas content and composition, etc... What we are claiming is simple is the experimental setup once the correct parameters are identified.

¹⁶ Actually, the degassing part is quite important. We focus on it elsewhere.

Back to the experimental setup. The typical driving pressure relevant to SBSL (~ 1.5 atm) is too small to cause bubbles to form spontaneously in the flask [1]. Instead, the bubble is usually seeded somehow. In the original work of Gaitan, an air bubble was injected using a needle and syringe through a small hole in the flask's seal [7]. More recently, seeding methods involve shooting a small jet of water into the flask (like our shrimp friends!) or blasting the water with a laser to boil a small volume [2]. The later method is preferred as it enables more precise control over the initial bubble's radius. The small bubbles formed this way coalesce at the center of the flask into a single, stable bubble [3].

Now that we know about how single, stable bubbles are formed in the lab, we can discuss a number of quantities of experimental interest. The bubble's radius may be measured by *Mie scattering* [4]. We may also analyze light spectrum which contains information on the bubble's contents: in principle, we can learn about the temperature inside the bubble and spectral lines contain information on the matter [5]. As we will see, it is actually not so simple to understand the light spectrum [6]. ...

what conditions are necessary for light emission (i.e. what is the phase space [9]) (Ar content, driving frequency, P_{max})

[7] has good discussion of early experimental errors. Measuring phase of SL relative to the acoustic field was an early attempt to explain SL. Phase here means how far in time is the SL light emission offset from the driven pressure. In the case of periodic oscillations, this is a phase. A handful of early models assumed that the light emission occurred during expansion of the bubble. Others assumed that it was at some point during. Most of these were ruled out when it was observed that the light emission is for a very short duration near maximum compression, though the phase depends quite a bit on the initial bubble radius, the driving frequency, the resonances of the flask, the physical properties of the liquid, etc [5; 7]. These complicated relationships were unknown to the early investigators of SL and were quite difficult to measure in MBSL. For this reason, it wasn't until SBSL was discovered that many of these models were dismissed [7]. In this paper, they present the discovery of SBSL...

IV. LET THERE BE LIGHT!

A. The Plasma

B. Brehmasstunglingnls

C. Recombination

D. Electronic transitions

V. SUMMARY

VI. ACKNOWLEDGMENTS

Appendix A: The Navier-Stokes Equations

The Rayleigh-Plesset (RP) equation can be deduced from the Navier-Stokes equations [5; 10; 22; 29; 30; 31]. To that end, we remind ourselves of the Navier-Stokes equations here.

The *total* change (in time) of mass in an arbitrary element of a fluid (whose coordinates and boundary may depend on time) is given by $\frac{d}{dt} \int_{\Omega_t} \rho dV$ where Ω_t is the domain of the fluid element under consideration and $\rho(\mathbf{x}, t)$ is the local, time-dependent density of the fluid. Using the transport theorem of fluid dynamics [58], Gauss's theorem, and (with only some loss of generality) taking Ω_t to be a *fluid parcel* (so that the boundary of the fluid parcel, $\partial\Omega_t$, moves with the fluid's velocity, $\mathbf{u}(\mathbf{x}, t)$), this becomes

$$\frac{d}{dt} \int_{\Omega_t} \rho dV = \int_{\Omega_t} \partial_t \rho dV + \int_{\partial\Omega_t} \rho \mathbf{u} \cdot \mathbf{n} dA = \int_{\Omega_t} \partial_t \rho + \nabla \cdot (\rho \mathbf{u}) dV. \quad (\text{A1})$$

Now to have *mass-continuity*, which we will require on physical grounds, we set eq. A1 to 0. Basically, we are saying no additional material is being added or removed from the fluid. Since the fluid parcel's boundary Ω_t is arbitrary, we find that $\partial_t \rho + \nabla \cdot (\rho \mathbf{u}) \equiv 0$ which is true for every point in the fluid volume.

Newton's second law for fluids (*momentum-continuity*) is defined similarly [58; 59]. We write the momentum-density as $\rho \mathbf{u}$ with momentum given by $\int_{\Omega_t} \rho \mathbf{u} dV$. To simplify what follows, we focus on only the i^{th} component of velocity

at a time. Then Newton's second law can be written as

$$\frac{d}{dt} \int_{\Omega_t} \rho u_i dV = \int_{\Omega_t} \partial_t(\rho u_i) dV + \int_{\partial\Omega_t} \rho u_i (\mathbf{u} \cdot \mathbf{n}) dA = F_i. \quad (\text{A2})$$

Now using Gauss's theorem, the product rule, and mass-continuity we find $\frac{d}{dt} \int_{\Omega_t} \rho u_i dV = \int_{\Omega_t} \rho \frac{du_i}{dt} dV = F_i$. In vector notation this reads

$$\int_{\Omega_t} \rho \frac{d\mathbf{u}}{dt} = \mathbf{F} \quad (\text{A3})$$

We now turn to the forces. Let us separate the forces into *body-* and *surface-forces*: $\mathbf{F} = \int_{\Omega_t} \mathbf{f}_B dV + \int_{\partial\Omega_t} \mathbf{f}_S dA$. The body-force density, \mathbf{f}_B , is due to forces acting in the bulk of the liquid e.g. gravity, electrostatic forces, etc. and is typically from sources external to the liquid. We won't be concerned with these forces here. Instead, let us concentrate on the surface part. If we only consider an ideal fluid, the surface part can be written as $\int_{\partial\Omega_t} \mathbf{f}_S dA = - \int_{\partial\Omega_t} p \mathbf{n} dA = - \int_{\Omega_t} \nabla p dV$ with p the pressure and the minus sign being due to the sign convention: *out* of the surface $\partial\Omega_t$ is positive.

If instead the fluid is real, we can't neglect viscous forces. We suppose that the viscous surface term can be represented by a tensor, $\hat{\boldsymbol{\tau}}$ such that $\mathbf{F}_v = \int_{\partial\Omega_t} \hat{\boldsymbol{\tau}} \cdot \mathbf{n} dA = \int_{\Omega_t} \nabla \cdot \hat{\boldsymbol{\tau}} dV$. (Note, here the dot product is to be understood as matrix multiplication). To leading order in gradients of the velocity, (and under the physical constraints that the tensor be symmetric), the viscous-stress tensor is $\hat{\boldsymbol{\tau}} = \hat{\boldsymbol{\mu}} \cdot \hat{\boldsymbol{\epsilon}}$ where $\hat{\boldsymbol{\mu}}$ is the viscosity-tensor and $\hat{\boldsymbol{\epsilon}}$ is the strain-rate tensor: $\epsilon_{ij} = \frac{1}{2} [\partial_i u_j + \partial_j u_i]$.

In general, $\hat{\boldsymbol{\mu}}$ is a symmetric rank-4 tensor. However, if we assume an isotropic fluid¹⁷, we find that the viscous-stress tensor can be separated into two irreducible parts: a scalar, $\hat{\boldsymbol{\epsilon}}^{(v)}$, and traceless symmetric part, $\hat{\boldsymbol{\epsilon}}^{(s)}$ [60; 61]:

$$\begin{aligned} \hat{\boldsymbol{\tau}} &= \xi \hat{\boldsymbol{\epsilon}}^{(v)} + \mu \hat{\boldsymbol{\epsilon}}^{(s)} \\ \hat{\boldsymbol{\epsilon}}^{(v)} &= \delta_{ij} \epsilon_{kk} \\ \hat{\boldsymbol{\epsilon}}^{(s)} &= \hat{\boldsymbol{\epsilon}} - \frac{1}{3} \delta_{ij} \epsilon_{kk}. \end{aligned} \quad (\text{A4})$$

Thus, we see that the viscosity-tensor only has two free components: ξ , the normal viscosity and μ the shear viscosity. It is usual to combine the pressure (i.e. elastic-stresses) and the viscous-stresses into the stress-tensor $\hat{\boldsymbol{\sigma}} = -p \hat{\mathbf{I}} + \xi \hat{\boldsymbol{\epsilon}}^{(v)} + \mu \hat{\boldsymbol{\epsilon}}^{(s)}$. Combined with this, Newton's second law becomes

$$\int_{\Omega_t} \rho \frac{d\mathbf{u}}{dt} - \mathbf{F} = \int_{\Omega_t} \rho \frac{d\mathbf{u}}{dt} - \nabla \cdot \hat{\boldsymbol{\sigma}} - \mathbf{f}_B dV = 0 \quad (\text{A5})$$

Again, since we allow the volume of integration to be arbitrary, the integrand must vanish everywhere: $\rho \frac{d\mathbf{u}}{dt} - \nabla \cdot \hat{\boldsymbol{\sigma}} - \mathbf{f}_B = 0$. This is the momentum-continuity equation for a fluid. Now we would rather have this explicitly in terms of the velocity \mathbf{u} . To that end, we may substitute eq. A4 into the momentum-continuity equation. For e.g. the i^{th} component we may expand out the divergence part as

$$(\nabla \cdot \hat{\boldsymbol{\sigma}})_i = -\partial_i p + \left[\xi + \frac{2}{3} \mu \right] \partial_i (\nabla \cdot \mathbf{u}) + \mu \nabla^2 u_i \equiv -\partial_i p + \eta \partial_i (\nabla \cdot \mathbf{u}) + \mu \nabla^2 u_i \quad (\text{A6})$$

where we have introduced the *bulk-viscosity* $\eta = \xi + \frac{2}{3} \mu$. Collecting all of the components into vector form and, combined with the mass-continuity equation A1, we arrive at the *Navier-Stokes* (NS) equations for a compressible fluid:

$$\begin{aligned} \rho \frac{d\mathbf{u}}{dt} &= \rho [\partial_t \mathbf{u} + (\mathbf{u} \cdot \nabla) \mathbf{u}] = -\nabla p + \eta \nabla (\nabla \cdot \mathbf{u}) + \mu \nabla^2 \mathbf{u} + \mathbf{f}_B \\ \partial_t \rho + \nabla \cdot (\rho \mathbf{u}) &= 0. \end{aligned} \quad (\text{A7})$$

Some comments are in order. The total-derivative of a moving fluid $\frac{d}{dt} \equiv D_t$ is sometimes called the *material derivative*. In the case of velocity $D_t \mathbf{u}$ is the *acceleration* of the fluid. It records not only explicit time dependence of

¹⁷ Definitely true for water which has been frequently used in sonoluminescence experiments.

the fluid's velocity $\partial_t \mathbf{u}$ but also how the fluid's velocity varies *in space* as it moves past us: $(\mathbf{u} \cdot \nabla) \mathbf{u}$. The pressure term on the right hand side is to be understood as forces from the *elastic* energy. On the other hand, the terms $\sim \mathbf{u}$ are viscous terms that tend to make the velocity field spatially uniform: they vanish when the (spatial) derivatives of the velocity vanish. The bulk-viscosity term $\sim \eta$ damps radial changes in the fluids velocity (e.g. dilation/contraction) while the shear-viscosity term $\sim \mu$ resists shearing. The body term \mathbf{f}_B is from external sources. It is worth noting that solving eqs. A7 is a formidable task¹⁸ and is usually done using computers.

Appendix B: Electrical Arguments

Appendix C: The Casimir Argument

¹⁸ In fact, it's not even clear that the NS equations *can* be solved even for incompressible fluids. In 2000, it was announced that proving smooth, sensible solutions exist earns \$1,000,000 [62]. Better hurry though... inflation was 6.8% in Nov. 2021.

REFERENCES

- [1] M. Versluis, B. Schmitz, A. Von der Heydt, and D. Lohse, *Science* **289**, 2114 (2000).
- [2] D. Lohse, B. Schmitz, and M. Versluis, *Nature* **413**, 477 (2001).
- [3] X. Tang and D. Staack, *Science advances* **5**, eaau7765 (2019).
- [4] F. A. Everest, R. W. Young, and M. W. Johnson, *The Journal of the Acoustical Society of America* **20**, 137 (1948).
- [5] M. P. Brenner, S. Hilgenfeldt, and D. Lohse, *Reviews of modern physics* **74**, 425 (2002).
- [6] L. A. Crum and R. A. Roy, *Science* **266**, 233 (1994).
- [7] D. F. Gaitan, L. A. Crum, C. C. Church, and R. A. Roy, *The Journal of the Acoustical Society of America* **91**, 3166 (1992).
- [8] D. F. Gaitan, *An experimental investigation of acoustic cavitation in gaseous liquids*, Ph.D. thesis, The University of Mississippi (1990).
- [9] D. Lohse, *Physical review fluids* **3**, 110504 (2018).
- [10] K. S. Suslick and D. J. Flannigan, *Annu. Rev. Phys. Chem.* **59**, 659 (2008).
- [11] J. Schwinger, *Proceedings of the National Academy of Sciences* **90**, 958 (1993).
- [12] C. Eberlein, *Physical Review Letters* **76**, 3842 (1996).
- [13] S. Liberati, M. Visser, F. Belgiorno, and D. Sciamia, *Journal of Physics A: Mathematical and General* **33**, 2251 (2000).
- [14] V. Borisenok and S. Y. Sedov, *Physics of Atomic Nuclei* **83**, 1575 (2020).
- [15] D. J. Flannigan and K. S. Suslick, *The Journal of Physical Chemistry B* **117**, 15886 (2013).
- [16] D. J. Flannigan and K. S. Suslick, *The journal of physical chemistry letters* **3**, 2401 (2012).
- [17] V. A. Tatartchenko *et al.*, *Optics and Photonics Journal* **7**, 27 (2017).
- [18] N. Marinesco and J. Trillat, *Proceedings of the Royal Academy of Science* **196**, 858 (1933).
- [19] H. Frenzel and H. Schultes, *Zeitschrift für Physikalische Chemie* **27**, 421 (1934).
- [20] S. Li, C. E. Brennen, and Y. Matsumoto, *Introduction for amazing (cavitation) bubbles* (2015).
- [21] L. Rayleigh, *On the pressure developed in a liquid during the collapse of a spherical cavity: Philosophical magazine series* **6**, 34, 94–98 (1917).
- [22] M. S. Plesset and A. Prosperetti, *Annual review of fluid mechanics* **9**, 145 (1977).
- [23] B. P. Barber, R. Hiller, K. Arisaka, H. Fetterman, and S. Putterman, *The Journal of the Acoustical Society of America* **91**, 3061 (1992).
- [24] B. P. Barber and S. J. Putterman, *Nature* **352**, 318 (1991).
- [25] C. Wu and P. H. Roberts, *Physical review letters* **70**, 3424 (1993).
- [26] H. P. Greenspan and A. Nadim, *Physics of Fluids A: Fluid Dynamics* **5**, 1065 (1993).
- [27] R. Hiller, S. J. Putterman, and B. P. Barber, *Physical review letters* **69**, 1182 (1992).
- [28] B. Gompf and R. Pecha, *Physical Review E* **61**, 5253 (2000).
- [29] A. Prosperetti, *Sonochemistry and sonoluminescence*, 39 (1999).
- [30] A. Prosperetti and A. Lezzi, *Journal of Fluid Mechanics* **168**, 457 (1986).
- [31] K. Yasui, *Acoustic cavitation and bubble dynamics* (Springer, 2018).
- [32] C. E. Brennen, *Cavitation and bubble dynamics* (Cambridge University Press, 2014).
- [33] M. S. Plesset, (1949).
- [34] J. D. Jackson, *Classical electrodynamics* (1999).
- [35] T. Leighton, (2007).
- [36] J. B. Keller and M. Miksis, *The Journal of the Acoustical Society of America* **68**, 628 (1980).
- [37] A. Lezzi and A. Prosperetti, *Journal of Fluid Mechanics* **185**, 289 (1987).
- [38] A. Prosperetti, L. A. Crum, and K. W. Commander, *The Journal of the Acoustical Society of America* **83**, 502 (1988).
- [39] J. B. Keller and I. I. Kolodner, *Journal of applied physics* **27**, 1152 (1956).
- [40] K. Yasui, in *Sonochemistry and the Acoustic Bubble* (Elsevier, 2015) pp. 41–83.
- [41] R. Löfstedt, K. Weninger, S. Putterman, and B. P. Barber, *Physical Review E* **51**, 4400 (1995).
- [42] B. P. Barber, R. A. Hiller, R. Löfstedt, S. J. Putterman, and K. R. Weninger, *Physics Reports* **281**, 65 (1997).
- [43] K. Weninger, R. Hiller, B. P. Barber, D. Lacoste, and S. J. Putterman, *The Journal of Physical Chemistry* **99**, 14195 (1995).
- [44] R. Hiller, K. Weninger, S. J. Putterman, and B. P. Barber, *Science* **266**, 248 (1994).
- [45] D. Lohse, M. P. Brenner, T. F. Dupont, S. Hilgenfeldt, and B. Johnston, *Physical review letters* **78**, 1359 (1997).
- [46] D. J. Flannigan and K. S. Suslick, *Nature* **434**, 52 (2005).
- [47] D. J. Flannigan, S. D. Hopkins, C. G. Camara, S. J. Putterman, and K. S. Suslick, *Physical review letters* **96**, 204301 (2006).
- [48] Y. An and C. Li, *Physical Review E* **80**, 046320 (2009).
- [49] Y. An and C. Li, *Physical Review E* **78**, 046313 (2008).
- [50] Y. An, *Physical Review E* **74**, 026304 (2006).
- [51] S. Sivasubramanian, A. Widom, and Y. Srivastava, *arXiv preprint cond-mat/0207465* (2002).
- [52] R. Löfstedt, B. P. Barber, and S. J. Putterman, *Physics of Fluids A: Fluid Dynamics* **5**, 2911 (1993).
- [53] W. Lentz, A. A. Atchley, and D. F. Gaitan, *Applied optics* **34**, 2648 (1995).
- [54] V. Bjerknes, *Die Kraftfelder*, Vol. 28 (F. Vieweg, 1909).
- [55] T. J. Matula, *Ultrasonics* **38**, 559 (2000).
- [56] T. J. Matula, S. M. Cordry, R. A. Roy, and L. A. Crum, *The Journal of the Acoustical Society of America* **102**, 1522

- (1997).
- [57] T. J. Matula, Philosophical Transactions of the Royal Society of London. Series A: Mathematical, Physical and Engineering Sciences **357**, 225 (1999).
 - [58] J. M. McDonough, (2009).
 - [59] L. Schoeffel, arXiv preprint arXiv:1407.3162 (2014).
 - [60] A. Zee, *Group theory in a nutshell for physicists*, Vol. 17 (Princeton University Press, 2016).
 - [61] L. Landau and E. Lifshitz, Course of Theoretical Physics **6** (1987).
 - [62] C. L. Fefferman, The millennium prize problems **57**, 22 (2006).